GMSK Co-Channel Demodulation

D.J. Nelson and J.R. Hopkins
National Security Agency
Ft. Meade, MD 20755, USA

ABSTRACT

Gaussian Minimum Shift Keying (GMSK) is a modulation method used by GSM phone networks and the Automatic Identification System (AIS) used by commercial ships. Typically these systems transmit data in short bursts and accomodate a large number of users by time, frequency and power management. Co-channel interference is not a problem unless the system is heavily loaded. This system load is a function of the density of users and the footprint of the receiver. We consider the problem of demodulation of burst GMSK signals in the presence of severe noise and co-channel interference. We further examine the problem of signal detection and blind estimation and tracking of all of the parameters required in the demodulation process. These parameters include carrier frequency, carrier phase, baud rate, baud phase, modulation index and the start and duration of the signal.

Keywords:GMSK, GSM, AIS, co-channel interference, demodulation, Viterbi decoding, carrier estimation

1. INTRODUCTION

Gaussian Minimum Shift Keying (GMSK) is a modulation method used by GSM phone networks and the Automatic Identification System (AIS) used by commercial ships. Typically these systems transmit data in short bursts and accomodate a large number of users by time, frequency and power management. Co-channel interference is not a problem unless the system is heavily loaded. This system load is a function of the density of users and the footprint of the receiver. We consider the problem of demodulation of burst GMSK signals in the presence of severe noise and co-channel interference. We further examine the problem of signal detection and blind estimation and tracking of all of the parameters required in the demodulation process. These parameters include carrier frequency, carrier phase, baud rate, baud phase, modulation index and the start and duration of the signal.

GSM is a common cell phone standard used in much of the world. AIS is a system used for collision avoidance and is mandated on all large commercial ships. The AIS and GSM signals are similar in the sense that they are both time division (TDM) multiplexed, transmitting data in short bursts within a narrow time slot [1, 2]. In addition, the GSM signal is frequency division multiplexed (FDM). The GSM signal is transmitted in a time-frequency slot allocated by the ground station, where the assigned frequency is used to avoid conflicts with nearby cells, and the the time slot assignment is assigned to minimize conflicts with other users within the cell. Power management is used to further minimize conflicts. TDM, FDM, and power management make it possible for a large number of users to share the same transmission band.

Unlike GSM, the AIS signal is self organizing in the sense that each ship selects a relatively clear time slot in which to transmit. Power management is not used in the AIS system, since, in the expected density of ships within the approximate 25 mile line of sight range may be expected to be small. Near port, or in dense shipping lanes, such as the Mediterranean, signals received by land or airborne receivers may observe a much higher signal density. In these situations, co-channel interference may be a significant problem.

The methods we present are based on a signal model that is subtly different from the standard model in the literature. MSK and GMSK signals are normally represented as the sum of pulse amplitude modulation (PAM) signals representing the frequencies of individual transmitted bits [3]. The model we present is more intuitive and is based on a PAM representation of the instantaneous frequency of the entire signal. Kaleh uses the conventional representation to give a reduced complexity MLSE demodulator that provides near-optimal performance in Gaussian noise [4]. Kaleh's process is based on matched filters and uses Viterbi decoding to determine the most likely transmitted bit stream. Saulnier reduces the number of matched filters to further reduce the complexity [5]. The matched filters in these processes are based on the conventional signal model.

Mathematics for Signal and Information Processing, edited by Mark S. Schmalz, Gerhard X. Ritter, Junior Barrera, Jaakko T. Astola, Franklin T. Luk, Proc. of SPIE Vol. 7444, 74440V · © 2009 SPIE
CCC code: 0277-786X/09/$18 · doi: 10.1117/12.825196

Based on our signal model, we present a matched filter demodulation process. The filters in our process are completely different from previous processes. However, the conventional signal model and our signal model may be seen to be completely equivalent.

Laster compares twenty-five non-coherent and two coherent demodulators [6]. In the case of co-channel interference and additive white Gaussian noise, he concludes that coherent demodulation is preferred. The methods we present represent such a coherent demodulation process. The focus of most previous efforts has been to reduce the computational complexity for efficient implementation on a fixed point DSP chip [3]-[8]. We do not address the issue of DSP implementation, since we only require efficient implementation on a general purpose computer. This simplifies the problem since machine precision and complex arithmetic are not issues.

The problem of co-channel interference has been addressed somewhat in the literature. Halonen, *et al.* present a joint, simultaneous demodulation of the signal and interference [8]. While this may be desirable, we follow a less complicated approach of first demodulating the stronger signal. This requires the estimation of fewer parameters and results in a less cumbersome trellis in the Viterbi decoding. In addition, we do not need to make any assumptions about the relative baud phases of the two signals.

Estimation of signal parameters has not been well addressed in the literature. We present methods based on cross-spectral methods we have previously presented for other applications [9]-[11]. These methods provide efficient and accurate blind estimation of all signal parameters needed for GMSK demodulation.

2. THE SIGNAL MODEL

2.1. Minimum Shift Key (MSK) Modulation

We first discuss MSK modulation from which GMSK modulation is derived. We model the signal by first assuming a bit stream, $< b_0 \dots b_{N-1} >$, $b_n \in \{0, 1\}$. The bit stream is used to generate a pulse amplitude Modulated (PAM) signal

$$p(t) = \sum_n (-1)^{b_n+1} I_n(t), \tag{1}$$

where $I_n(t) = 1$ on the interval $[nT_B, (n+1)T_B)$ and is zero elsewhere. In this representation, T_B is the baud length of the signal, and the baud rate is $f_B = 1/T_B$. It is convenient to use the angular frequency notation in which f (Herz), is converted to angular frequency, ω (radians), by $\omega = 2\pi f$.

The desired baseband instantaneous frequency (IF) function of the MSK signal is constructed as

$$\omega_M(t) = \frac{\mu\omega_B}{2} p(t), \tag{2}$$

where $\mu = 1/2$ is the modulation index of the MSK signal and ω_B is the angular baud rate. The MSK phase function, $\phi_M(t)$, is produced by integrating $\omega_M(t)$, and the resulting baseband MSK signal is translated to the transmission frequency by the carrier frequency, ω_c, to produce a transmitted signal, $s_M(t)$.

$$\phi_M(t) = \int_0^t \omega_M(x)dx \tag{3}$$

$$s_M(t) = Ae^{i\omega_c} e^{i\phi_M(t)}, \tag{4}$$

where A is assumed to be constant. For $\mu = 1/2$, over the interval of one baud, the MSK phase function changes by $+\pi/2$ when the value of the transmitted bit is 1, and by $-\pi/2$ when the value of the transmitted bit is 0.

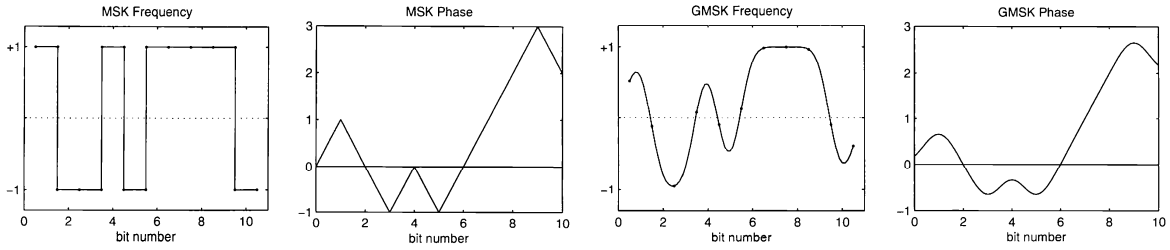

(a) MSK IF $\omega_M(t)$ (b) MSK phase $\phi_M(t)$ (c) GMSK IF $\omega_G(t)$ (d) GMSK phase $\phi_G(t)$

Figure 1. GMSK IF and phase functions

2.2. Gaussian MSK (GMSK) Modulation

Construction of the GMSK signal is similar to that of the MSK signal. The MSK baseband IF, $\omega_M(t)$, is generated, and a Gaussian filter, $G(t)$, is applied to produce the GMSK baseband IF. The rest of the construction is as in MSK

$$\omega_G(t) = \int \omega_M(x)G(t-x)dx \tag{5}$$

$$\phi_G(t) = \int_0^t \omega_G(x)dx \tag{6}$$

$$s_G(t) = Ae^{i\omega_c}e^{i\phi_G(t)}. \tag{7}$$

The Gaussian filter reduces the signal bandwidth at the expense of inter symbol interference. For GMSK signals, each symbol only experiences significant interference from the immediately adjacent symbols.

The model we have presented differs subtly from the conventional model in which a GMSK signal, $\tilde{s}_{nG}(t)$, is generated for each transmitted bit. The transmitted signal, $\tilde{s}_G(t)$, is then produced as the sum of time translations of these signals

$$\tilde{s}_G(t) = \sum_n \tilde{s}_{nG}(t + nT_B) \tag{8}$$

Since convolution and summation commute, the two models are equivalent (*i.e.* $s_G(t) \equiv \tilde{s}_G(t)$.) In either case, the GMSK signal may be described as a constant-modulus continuous-phase Gaussian-"filtered" FSK signal with modulation index of 1/2. For the bit stream, $< 0, 1, 1, 0, 1, 0, 0, 0, 0, 1 >$, the signals, $\omega_M(t)$, $\phi_M(t)$, $\omega_G(t)$ and $\phi_G(t)$ are displayed in Fig. 1.

2.3. Received Co-channel signals

We assume a short duration burst GMSK signal in the presence of noise and co-channel interference. We assume that the baud rate is known, but none of the other signal parameters are known with sufficient accuracy to demodulate the signal. The problem is to recover required signal parameters and demodulate the signal. For the collision of two signals, the received signal has the representation

$$S(t) = s_1(t-\delta_1) + s_2(t-\delta_2) + \eta(t) \tag{9}$$

$$s_i(t) = A_i e^{i(\omega_{ic}(t)+\phi_i)}e^{i\phi_{iG}(t+\delta_i)} \tag{10}$$

where $s_i(t)$ are GMSK signals with amplitudes, A_i, unknown time delays, δ_i, and unknown carrier frequencies, $\omega_{c_i}(t)$. We must recover these parameters, as well as the baud phase and the modulation index.

A received 9600 baud signal in 3 dB co-channel interference is represented in Fig. 2. The interfering signal also has a baud rate of 9600, with a 3 kHz carrier frequency offset from the stronger signal. In the absence of noise and interference, GMSK signals have constant modulus. As this example shows, this is not the case for signals in interference.

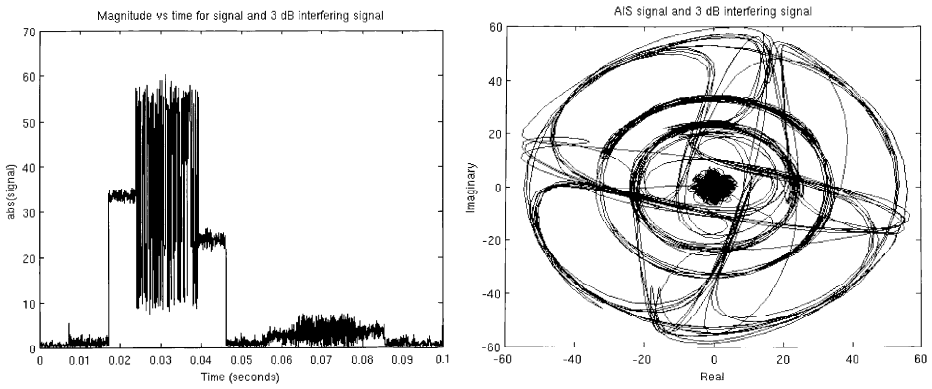

Figure 2. Received signal in 3dB co-channel interference Left: signal magnitude; Right: Complex signal

3. POLY-BIT MATCHED FILTER GMSK DEMODULATION

Kaleh, Saulnier and possibly others have proposed matched filter demodulation based on the model Eq. (8) [4, 5]. We now derive matched filters based on the model Eq. (7) and demonstrate a simple demodulation method. The filters we present are not the same as previously presented filters.

For this discussion, we assume a baseband GMSK signal, $s(t)$, with no carrier drift and known baud rate and modulation index. We discuss in a later section the processes by which signal parameters may be estimated to properly baseband the signal. For any M-bit sequence $\beta =< b_0 \dots b_{M-1} >$, we may generate a filter, $F_\beta(t)$, matched to the signal of interest, by simply applying the GMSK modulation process described in section 2 to that bit sequence. For MSK modulation, any portion of the signal representing the same bit sequence as the filter will differ from the filter by only a constant phase and gain. For GMSK, this true, except for the effects of inter-symbol interference, primarily near the ends of the filter.

For demodulation, we construct a bank of poly-bit filters. For M-bit filters, the bank consists of 2^M filters, $F_m(t)$, representing all possible binary patterns (states) of length M. We index these filters by the integer equivalent of the binary pattern they represent. In principle, the filters may be generated with any length. In testing, it was determined that a filter length of MT_B is nearly optimal. For tri-bit filters and signals sampled at eight times the baud rate, the bank of filters consists of eight filters of length 24. Preamble and postamble filters may be similarly constructed.

In constructing the matched filters, there is an arbitrary carrier phase. For reasons that will be clear in the Viterbi decoding section, we construct all filters so that the argument of the filter at the center is zero. For a filter, F_n of length, L, this requires that $\arg\{F_n(L/2)\} = 0$.

3.1. Applying Filters

We assume that $s(t)$ is a baseband signal and apply the filters by cross-correlating each filter with the signal

$$R_m(T) = \int s(t+T)F_m^*(t)dt. \tag{11}$$

This process may be implemented by fast frequency domain convolution methods.

3.2. Estimating Baud Phase

We must next estimate a baud phase representing the location of the center of each baud. Since we assume a stable baud rate and a signal sampled at an integer multiple of the baud rate, we need only estimate an ensemble average of the baud phase. We first estimate the maximum correlation magnitude function

$$M(T) = \max_m |R_m(T)| \tag{12}$$

We accumulate $M(T)$ to estimate an ensemble baud phase

$$\bar{M}(\tau) = \sum_k M(kT_B + \tau) \quad , \tau \in [0, T_B) \tag{13}$$

The estimated ensemble baud phase and baud centers are

$$\Phi_B = \arg\max_\tau \bar{M}(\tau) \tag{14}$$

$$C_n = nT_B + \Phi_B \tag{15}$$

3.3. Estimating the Correlation Array

The correlation array is estimated as

$$\mathcal{R}_{m,n} = R_m(C_n) \tag{16}$$

This array represents the correlation of the signal with each of the matched filters, evaluated at the estimated baud centers. The row index is the matched filter index, and the column index is a baud (time) index of the transmitted bit.

There is only one correct poly-bit sequence. For example the correct tri-bit sequence for the binary sequence, 0110100001, is 011 110 101 010 100 000 000 001, in that order. If we know the correct sequence, m_n, of poly-bits, we can correctly recover the transmitted bit sequence and conversely.

3.4. Estimating Constellation Orientation

As previously noted, the signal phase for an MSK signal is expected to change by $\pm\pi/2$ over each baud interval. Our matched filters have zero central phase and we may assume that the correlation array, $\mathcal{R}_{m,n}$ represents the correlation values at the baud centers, when the filters are properly aligned. If we knew the correct sequence of poly-bits, m_n, representing the data, the correlation sequence, $\mathcal{R}_{m_n,n}$, has the expected properties that

$$\mathrm{E}\{\arg\{\mathcal{R}_{m_n,n}\}\} = k_n \frac{\pi}{2} + \phi_c \tag{17}$$

$$\mathrm{E}\{\arg\max_m\{|\mathcal{R}_{m,n}|\}\} = m_n \tag{18}$$

for integers, k_n, and unknown initial carrier phase, ϕ_c. It must be emphasized that these are expected values. If there is significant noise or interference, it is not sufficient to estimate ϕ_c from one observation. We may combine these observations from the entire data sequence to estimate the initial carrier phase, $\phi_c|_{\pi/2}$, where $|_x$ represents the remainder after division by x. To do this, we estimate the poly-bit sequence, m_n, by Eq. (18) and estimate ϕ_c by averaging the correlation sequence

$$\phi_c \approx \arg\{\mathrm{mean}(|\mathcal{R}_{m_n,n}|e^{i\arg\{\mathcal{R}_{m_n,n}\}|_{\pi/2}})\}. \tag{19}$$

For a GMSK signal in moderate co-channel interference, this process is demonstrated in Fig. 4. A scatter plot of all the entries of $\mathcal{R}_{m,n}$ is shown in Fig. 4a. This example signal has very weak interference for illustrative purposes, but the process does work for stronger interference. We see that the points with the largest magnitudes fall near each other in four groups spaced $\pi/2$ apart. These groups are shown in the constellation diagram in Fig. 4b. The constellations points are not located at multiples of $\pi/2$ because the initial carrier phase $\phi(0)$ is not zero. We recover and remove the initial carrier phase, as described above, as represented in Fig 4c. The phase adjusted scatter plot of the entire correlation matrix is shown in Fig. 4d.

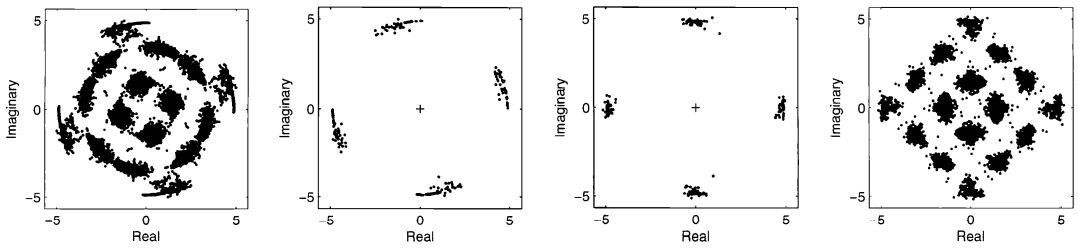

(a) Cross-correlation values (b) Constellation diagram (c) Phase drift removed (d) State scores

Figure 3. Reorienting the cross-correlation values to get state scores

3.5. Poly-bit State Scores

Having reoriented the constellation into a known configuration and removing any carrier estimation error we calculate the state scores using the cross-correlation matrix values. As stated, the matched filter states that correlate best have large magnitude and now have expected phase, $n\pi/2$. In other words, the correct filter produces a cross-correlation that is nearly real or pure imaginary. One way to score each matched filter state by using the infinity norm

$$P_{m,n} = ||\mathcal{R}_{m,n}||_\infty = \max(|\Re\{\mathcal{R}_{m,n}\}|, |\Im\{\mathcal{R}_{m,n}\}|), \tag{20}$$

where $\Re$ and $\Im$ are the real and imaginary parts, respectively. This norm produces an array of state scores to which we may apply Viterbi decoding to recover the most likely state sequence.

If we cannot estimate the initial carrier phase, ϕ_c, the constellation cannot be stabilized in the correct orientation, and the best state score array we may obtain is

$$P_{m,n} = |\mathcal{R}_{m,n}| \tag{21}$$

4. VITERBI DECODING

The Viterbi decoding algorithm is an efficient method for determining the most likely state sequence in a hidden Markov Model (HMM), given a set of observations (*c.f.* [12, 13].) The basis of the algorithm is that the probability/likelihood of each path ending at a particular state as the product of the path probability into its previous state, the probability of transitioning from the previous state to the current state and the probability of the current state given the observation. The Viterbi algorithm discards all but the most likely path into each state, making it computationally and memory efficient.

GMSK modulation may be cast in terms of a hidden Markov model under our paradigm by letting each poly-bit pattern represent a state. If the signal transmits the M-bit sequence, β_k, centered at time index, n, then the signal is in state, k, at time, n. If M is odd, the transmitted bit stream may be recovered as the center bit of the poly-bits represented by the state sequence.

We may assign observation likelihoods of each poly-bit state at each time as the infinity norm, magnitude, or other function of the correlation array, $\mathcal{R}_{m,n}$, To estimate the state sequence likelihoods, we need the transition probability matrix. For tri-bits, if we are in the state $\beta_n =< b_1, b_2, b_3 >$, and the data are not biased, the next state is either $< b_2, b_3, 0 >$ or $< b_2, b_3, 1 >$, with equal probability, resulting in a transition probability matrix,

$\mathcal{T}_{k,m}$

	000	001	010	011	100	101	110	111
000	.5	.5	0	0	0	0	0	0
001	0	0	.5	.5	0	0	0	0
010	0	0	0	0	.5	.5	0	0
011	0	0	0	0	0	0	.5	.5
100	.5	.5	0	0	0	0	0	0
101	0	0	.5	.5	0	0	0	0
110	0	0	0	0	.5	.5	0	0
111	0	0	0	0	0	0	.5	.5

We assume a state model representing the 2^M M-bit patterns indexed by their integer equivalent. Let $p_{k,m}(n)$ be the likelihood of the path into state, k, at time, $n-1$, and terminating at state, m, at time, n. Let $\mathcal{P}_m(n)$ be the likelihood of the most likely path terminating at state, m, at time, n. We initialize by assuming that $\mathcal{P}_m(0) = 1/(2^N)$. We then have the relationship

$$p_{k,m}(n) = \mathcal{P}_k(n-1) \times \mathcal{T}_{k,m} \times P_{m,n} \tag{22}$$

where $P_{m,n}$ is the state likelihood array we have assigned, based on the correlation array, $\mathcal{R}_{m,n}$. We compute the most likely input states and path likelihoods at time, n

$$\mathcal{S}_m(n) = \arg\max_k p_{k,m}(n) \tag{23}$$

$$\mathcal{P}_m(n) = \max_k p_{k,m}(n) \tag{24}$$

At each iteration, only the most likely path into each state is retained, discarding all other paths. Finally, we can determine the most likely path (Viterbi path) by backtracking through $\mathcal{S}_m$ from the most likely final state. To prevent underflow likelihoods are usually represented as log likelihoods, and the propagation equations are applied as sums of logarithms of likelihoods rather than products of likelihoods.

5. IMPROVEMENT OPTIONS

The demodulator, described so far, is similar to other coherent MLSE demodulators using the Viterbi decoding and a bank of matched filters [4]. We wish to suggest several improvements to the demodulation process and give estimates on the performance of these in AWGN and co-channel interference. The main improvements are the use of a correlation phase states [14], increasing the order of the poly-bit model, and forcing the signal to have constant modulus.

5.1. Correlation Phase States

The demodulator that we have described uses the infinity norm of the reoriented constellation diagram as the score for the states in the Viterbi algorithm. This works since the carrier phase of each of the matched filters is 0. We now suggest that for each poly-bit state we define four additional phase states, $\mathfrak{S}_{m,n} \in \{0, \frac{\pi}{2}, \pi, 3\frac{\pi}{2}\}$. If the signal is in phase state, $j\frac{\pi}{2}$, at time, n, the only possible phase transitions are to states, $((j \pm 1)\frac{\pi}{2})|_{\pi/2}$. For each poly-bit state, we construct four separate matched filters, representing the possible phase states. It is not necessary to apply any additional filters. The extended correlation array may be computed from the original correlation array, $\mathcal{R}_{m,n}$, by projecting each coefficient onto the real and imaginary axes

$$\tilde{\mathcal{R}}_{4m+j,n} = \max(0, \Re\{\mathcal{R}_{m,n} e^{ij\frac{\pi}{2}}\}) \quad , j = 0, \ldots, 3 \tag{25}$$

The new model has four times as many states, and the phase states must be taken into account in constructing the transition probability matrix, but this model significantly out performs other models. The transition probability matrix has only two possible transitions from each state with equal probability.

5.2. Larger Order Poly-Bit Models

We have been careful to describe a system in which the order of the poly-bit model is arbitrary. The advantage of models of larger order is that the effects of inter-symbol interference are minimized, In addition, noise and co-channel interference decorrelate with the longer filters. Since the number of M-bit patterns is 2^M, the computational complexity grows as the square of the model order. The trade-off is the complexity of having to apply more filters. We have tested our process with models of order 3, 4 and 5 and present some results in the next section.

5.3. Forcing Constant Modulus

Clean GMSK signals have constant modulus. With addition of noise, interference and channel distortion, the received signal no longer has constant modulus. One option is to baseband the signal and then force it to have constant modulus by projecting the baseband signal onto the unit circle

$$\tilde{s}(t) = e^{i \arg\{s(t)\}}. \tag{26}$$

This process may not work well if the co-channel interference or noise cause the signal to loop around the origin. As long as the SNIR is above 1 dB, this will not be an issue. We have tested this option, and it generally improves performance.

6. PARAMETER ESTIMATION

For demodulation, we must know or estimate the burst location, the carrier frequency and phase and the baud rate and phase We now describe each of these parameters.

6.1. Finding the Data Burst

Fig. 2b is an example of the energy of a received signal containing four GMSK bursts. The first has fairly high SNR and should pose no problem for any demodulator. The second burst is has low SNR. Finally the last two bursts are partly overlapping in time, producing co-channel interference. We focus on demodulating overlapping bursts.

AIS signals have a known preamble and postamble indicating the start and end of the burst. This makes it possible to construct matched filters to find the burst boundaries, even in significant noise. Co-channel interference may be a problem, if the bursts are nearly simultaneous, and have nearly the same carrier frequency. If the carriers are sufficiently different, the matched filter approach is effective.

6.2. Baud Rate

Since the signal is transmitted in very short bursts, only a nominal estimate of the baud rate is required. We may assume that the baud rate is known and constant. We may also assume that the signal has been sampled at an integer multiple of the baud rate. In the discussion that follows, we assume a baud rate, $f_B = 9600$ bits-per-second (BPS) and a sample rate, $f_s = 8f_B = 76800$ Hz.

6.3. Estimation of Carrier Frequency and Modulation Index

We base carrier estimation and carrier tracking in the next subsection on cross-spectral representations of the signal. These representations and applications of them are covered in detail in [9]-[11]. We define the cross-spectral surface, $\mathbf{CIF}_{x,h}(\omega, T)$, by

$$\mathbf{CIF}_{x,h}(\omega, T) = \mathcal{S}_{x,h}(\omega, T + \frac{\epsilon}{2})\mathcal{S}^*_{x,h}(\omega, T - \frac{\epsilon}{2}) \tag{27}$$

$$\mathcal{S}_{x,h}(\omega, T) = \int h(-t)x(t+T)e^{-i\omega t}dt, \tag{28}$$

where $\mathcal{S}_{s,h}(\omega, T)$ is the short time Fourier transform (STFT) and $h(t)$ is a windowing function symmetric about zero. In all examples presented in this paper, a Hanning window was used. For constant T_0, $\mathcal{S}_{x,h}(\omega, T_0)$ reduces to the standard windowed Fourier transform. We define the cross-spectrum, $\mathbf{CS}_{x,h}(\omega)$, by

$$\mathrm{CS}_{x,h}(\omega) = \mathbf{CIF}_{x,h}(\omega, T_0), \tag{29}$$

where we drop T_0 from the notation under the assumption that T_0 and h are appropriately chosen to contain the portion of the signal we wish to analyze.

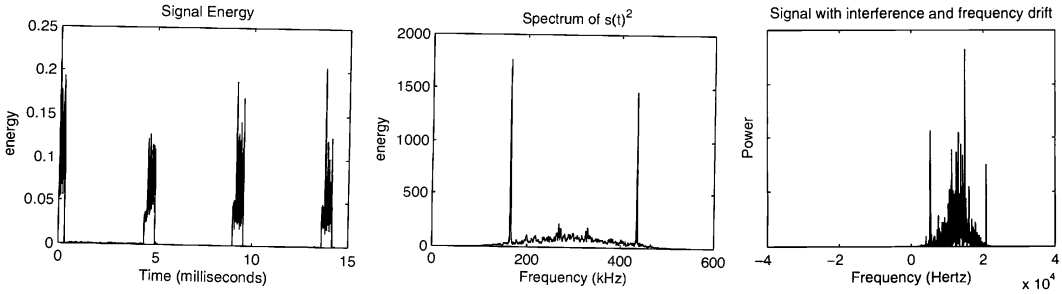

Figure 4. Left: GSM Signal envelop; Center: Power spectrum of squared GSM signal Right: Power spectrum of squared AIS signal in 3dB co-channel interference.

We may concentrate (reassign in frequency) the CIF surface at each time, T_0

$$\mathbf{C}_{x,h}(\Omega, T_0) = \sum_{\mathcal{A}(\omega,T_0)=\Omega} \mathbf{CIF}_{x,h}(\omega, T_0) \tag{30}$$

$$\mathcal{A}_{x,h}(\omega, T) = \arg\{\mathbf{CIF}_{x,h}(\omega, T)\} \tag{31}$$

Clearly we may apply the same process to the cross-spectrum.

We temporally simplify the discussion by assuming a clean MSK signal. To recover the carrier frequency, we note that squaring the complex signal results in a continuous phase FSK signal with modulation index, $\mu = 1$. It is easily verified that, the resulting signal is the sum to two sine waves, each multiplied by a step function

$$s^2(t) = p^+(t)e^{i(\omega_c + \frac{\omega_B}{2})t} + p^-(t)e^{i(\omega_c - \frac{\omega_B}{2})t}, \tag{32}$$

where $p^+(t) = \max(0, p(t))$ and $p^-(t) = \min(0, p(t))$. The tones at $\omega_c \pm \omega_B/2$ are observable in the spectrum of s^2.

The cross-spectral magnitude, $|\mathrm{CS}_{s^2,h}(\omega)|$, of a GMSK burst with drifting carrier and 3 dB co-channel interference, is shown in Fig. 3a. To eliminate false detection of carriers, candidate tone pairs, ω_1, ω_2, are identified in the cross-spectrum and validated. For $\mu = 1/2$ and angular baud rate, ω_B, valid pairs satisfy $|\arg\{\mathrm{CS}_{s^2,h}(\omega_2)\mathrm{CS}^*_{s^2,h}(\omega_1)\}| \approx \omega_B$.

We have assumed a modulation index, $\mu = 1/2$ and a known baud rate, f_B. If either of these assumptions is not true, tones at $\omega_c \pm \tilde{\omega}_B$ are still observed in the spectrum of $s^2(t)$, and the baud rate and modulation index are related by

$$\mu = \frac{\tilde{\omega}_c}{\omega_c}. \tag{33}$$

This relationship may be used to adjust the matched filters presented later.

6.4. Carrier Tracking

It is sometimes necessary to estimate and remove residual carrier drift. This drift may be estimated by methods of our previously cited work. For simplicity, we assume a clean MSK signal with drifting carrier. Using the

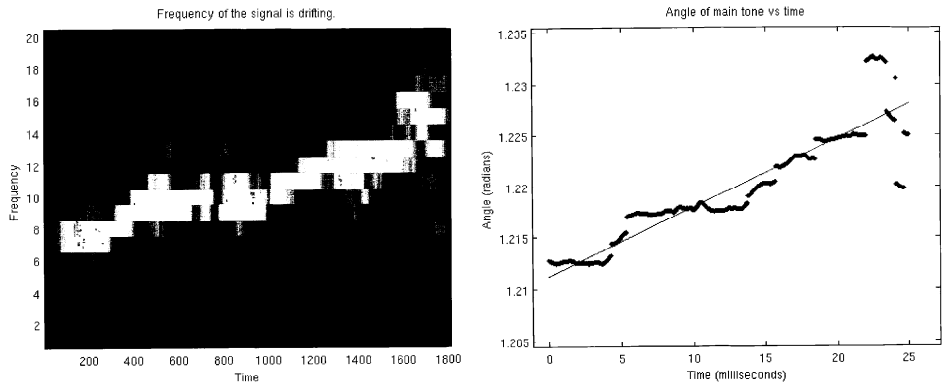

Figure 5. Basebanding the signal

methods of the previous section, we estimate the nominal average carrier, $\tilde{\omega}_c$, translate the signal to nominal baseband and square the signal

$$s_{\tilde{\omega}_c} = s(t)e^{-i\tilde{\omega}_c t} \tag{34}$$

$$s^2_{\tilde{\omega}_c}(t) \approx e^{i\omega_D(t)t}\left(p^+(t)e^{i\frac{\omega_B}{2}t} + p^-(t)e^{-i\frac{\omega_B(t)}{2}t}\right) \tag{35}$$

where $\omega_c = \tilde{\omega}_c + \omega_D(t)$ is the instantaneous carrier frequency, $\omega_D(t)$ is the residual carrier drift, and other functions and parameters are defined as in Eq. (32).

We concentrate the CIF surface to form the surface $\mathbf{C}_{s^2_{\tilde{\omega}_c},h}(\Omega, T)$, as described above. This process focuses the energy in the FSK "carriers". We then subtract $\omega_B/2$ from the argument of the positive frequency components and add $\omega_B/2$ to the argument of the negative frequency components

$$\tilde{\mathbf{C}}_{s^2_{\tilde{\omega}_c},h}(\Omega, T) = \mathbf{C}_{s^2_{\tilde{\omega}_c},h}(\Omega, T)e^{-i\frac{\Omega}{|\Omega|}\frac{\omega_B}{2}} \tag{36}$$

We peak-pick the surface $\tilde{\mathbf{C}}_{S^2_{\tilde{\omega}_c},h}(\Omega, T)$ at each time, T to recover the complex-valued component with the largest magnitude. The assumption is that the index of that component represents the frequency of the dominant FSK carrier, the magnitude represents the FSK carrier energy, and the argument provides an estimate of the instantaneous angular carrier drift function. To complete the process, a weighted polynomial fit is applied to the arguments of the peak sequence, where the weights are the peak magnitudes. Several curve fitting functions were tried, the best of which is the MATLAB robust fit function. An example of this process is shown in Fig. 3, where a synthesized AIS GMSK signal with carrier drift and 3 dB SIR co-channel interference was processed.

7. TESTING AND EVALUATION

The methods presented above were tested on synthesized AIS burst data. We present Monte Carlo results of 5-bit matched filter demodulation on these signals as a function of carrier offsets and co-channel SIR. The states for these tests consisted of 32 filter states and 4 phase states. The data for these tests were generated by a simulator that has been verified to accurately represent AIS signals. The signals were sampled at eight times the baud rate, which was assumed known at 9600 baud. No other signal parameters were assumed known. All signal parameters needed for demodulation were blindly estimated, and the signals were demodulated using these estimated parameters. The results of this series of tests are tabulated in Table 1. For SIR greater than 4 dB, there were no observed bit errors. The process was also tested for 3-bit matched filters (results not tabulated.) The 5-bit demodulation offered a significant advantage at low SIR, but for SIR greater than approximately 4 dB, the performance was nearly identical.

Carrier offset (Hertz)						
SIR	0	1000	2000	3000	4000	5000
0	35.62	29.49	23.02	11.50	5.30	0.04
1	28.94	24.18	15.13	8.83	2.29	0.00
2	11.47	12.43	7.66	4.42	0.36	0.00
3	0.47	2.52	1.87	0.86	0.00	0.00
4	0.01	0.16	0.08	0.05	0.00	0.00
5	0.00	0.00	0.00	0.00	0.00	0.00

Table 1. BER (%): co-channel interference, 5-bit demodulator using both constant modulus and phase states

REFERENCES

1. Cervera, M.A. and Ginesi, A., "On the Performance Analysis of a Satellite-based AIS System", *IEEE Workshop on Sig. Proc. for Space Comms.,* Oct. 2008, pp. 1-8.
2. http://www.navcen.uscg.gov/enav/ais/
3. Laurent, P.A., "Exact and Approximate Construction of Digital Phase Modulations by Superposition of Amplitude Modulated Pulses (AMP)",*IEEE Comm.Trans*, Feb. 1986,34(2), pp. 150-160.
4. Kaleh, G.K., "Simple Coherent Receivers for Partial Response Continuous Phase Modulation", *IEEE Jour. Selected Areas in Comm.*, Dec. 1989, 7(9), pp. 1427-1436.
5. Al-Dhahir, N. and Saulnier, G., "A High-Performance Reduced-Complexity GMSK Demodulator", *IEEE Comm. Trans.*, Nov. 1198, 46(11), pp. 1409-1412.
6. Laster, J.D., "Robust GMSK Demodulation Using Demodulator Diversity and BER Estimation", 1997, doctoral dissertation, VA Poly. Inst. and State Univ., Blacksburg, VA.
7. Souissi, M.G., Grati, K., Ghazel, A., and Kouki, A., "Software Efficient Implementaion of GMSK Modem for an Automatic Identification System Transciever", *IEEE Canadian Conf. on Elect. and Computer Eng.*, May 2008 ,pp. 601-606.
8. Halonen, T., Romero, J., Melero, J. *GSM, GPRS, and EDGE Performance: Evolution Towards 3G/UMTS*, 2003, John Wiley and Sons,Ltd., West Sussex, England, 2nd edn.
9. D. Nelson, "Special Purpose Correlation Functions",1989, internal report, (republished in part in: "Special Purpose Correlation Functions for Improved Parameter estimation and Signal Detection," *Proc. IEEE Conf. Acoust., Speech and Sig. Proc.*, Apr.,1993, Minneapolis, pp. 73-76).
10. Nelson, D.J.,"Cross-spectral methods for processing speech," Nov.2001, *J. Acoust.Soc.Am.*,110, 2575-2592.
11. Nelson, D.J., and Smith D.C., "A Linear Model for TF Distribution of Signals", Sept. 2006, *IEEE Sig. Proc. Trans.*, 54(9), pp. 3435-3447.
12. http://en.wikipedia.org/wiki/Viterbi_algorithm
13. Forney, G.D., "The Viterbi Algorithm", *Proc. of the IEEE*, Mar. 1973, 61(3), pp. 268-278.
14. Smith, D.C. and Nelson, D.J., "A comparison of two methods for demodulating a target AIS signal through a collision with an interfering AIS signal", (Aug. 2009), *SPIE Adv. Sig. Proc. Alg., Arch., and Imp. XIX*, (to appear).